Available online at www.sciencedirect.com
ScienceDirect
BioSystems 89 (2007) 166–172
BioSystems
www.elsevier.com/locate/biosystems

Ghost resonance in a pool of heterogeneous neurons

Pablo Balenzuela[a,b,1], Jordi Garcia-Ojalvo[a,*], Elías Manjarrez[c,2], Lourdes Martínez[c,2], Claudio R. Mirasso[d,3]

[a] *Departament de Física i Enginyeria Nuclear, Universitat Politècnica de Catalunya, Colom 11, E-08222 Terrassa, Spain*
[b] *Departamento de Física, Facultad de Ciencias Exactas y Naturales, Universidad de Buenos Aires, Pabellón 1, Ciudad Universitaria (1428), Buenos Aires, Argentina*
[c] *Instituto de Fisiología, Benemérita Universidad Autónoma de Puebla, 14 Sur 6301, Col. San Manuel, Apartado Postal 406, Puebla, Pue. CP 72570, México*
[d] *Departament de Física, Universitat de les Illes Balears, E-07122 Palma de Mallorca, Spain*

Received 12 December 2005; accepted 6 April 2006

Abstract

We numerically study the subharmonic response of a heterogeneous pool of neurons to a pair of independent inputs. The neurons are stimulated with periodic pulse trains of frequencies $f_1 = 2$ Hz and $f_2 = 3$ Hz, and with inharmonic pulses whose frequencies f_1 and f_2 are equally shifted an amount Δf. When both inputs are subthreshold, we find that the neurons respond at a frequency equal to $f_2 - f_1$ in the harmonic situation ($\Delta f = 0$), that increases linearly with Δf in the inharmonic case. Thus the neurons detect a frequency not present in the input; this effect is termed "ghost resonance". When one of the inputs is slightly suprathreshold the ghost resonance persists, but responses related with the frequency of the suprathreshold input also emerge. This behavior must be taken into account in experimental studies of signal integration and coincidence detection by neuronal pools.

Keywords: Neuronal dynamics; Neural coding; Signal integration; Coincidence detection; Pitch perception

1. Introduction

Coincidence detection is the simplest computational task faced by neuronal circuits. Recently, a simple coincidence detection mechanism has been proposed as the basis of binaural pitch perception in the human brain (Balenzuela and García-Ojalvo, 2005). By way of this mechanism, two periodic sound signals with different frequencies are applied to different ears (Pantev et al., 1996), and the pitch of the combined complex signal is detected psychoacoustically (Schouten et al., 1962). When the input signals are higher-order harmonics of an absent fundamental, the perceived tone is precisely that of the fundamental, in what's known as the "missing fundamental illusion". Since the perceived signal is not present in the input, the phenomenon has also been called "ghost resonance" (Chialvo, 2003).

In its original conception, ghost resonance was found for combinations of harmonic inputs (Chialvo et al., 2002), and as such was reported experimentally in lasers (Buldú et al., 2003; Van der Sande et al., 2005) and electronic circuits (Calvo and Chialvo, 2006). In the original excitable models considered (Chialvo et al., 2002) the input frequencies were on the order of Hz, much lower than the physiological conditions studied by Schouten et

* Corresponding author. Tel.: +34 93 739 8645; fax: +34 93 739 8000.
[1] Tel.: +54 11 4576 3390x817; fax: +54 11 4576 3357.
[2] Tel.: +52 22 22295500x7326; fax: +52 22 22295500x7323.
[3] Tel.: +34 971 172783; fax: +34 971 173426.
E-mail addresses: pbalen@gmail.com (P. Balenzuela), jordi.g.ojalvo@upc.edu (J. Garcia-Ojalvo), emanjar@siu.buap.mx (E. Manjarrez), celulula@hotmail.com (L. Martínez), claudio@galiota.uib.es (C.R. Mirasso).

0303-2647/$ – see front matter © 2006 Elsevier Ireland Ltd. All rights reserved.
doi:10.1016/j.biosystems.2006.04.014

al. (1962). Here we will consider input frequencies in the same order of magnitude, since we do not expect qualitative differences due to the different frequency range. Experiments in electronic circuits (Lopera et al., 2006) show that the phenomenon persists for frequencies in the kilohertz range.

When the inputs are distributed (Buldú et al., 2005), different neurons detect and transduce those harmonic signals into periodic pulse trains, which are transmitted further downstream through different pathways and processed by integrating units that must successfully detect the coinciding arrival of spikes, for the ghost resonance to occur. This behavior was studied in isolated-neuron models by Balenzuela and García-Ojalvo (2005). However, in real experimental situations (Manjarrez et al., 2006), the detecting and processing units do not consist of single neurons connected in one-to-one synapses, but in pools of heterogeneous neurons that respond in a diverse way to the complex distributed inputs, and whose collective behavior must be analyzed in detail before one is able to make reasonable predictions to be tested experimentally.

In this paper we model the response of a pool of neurons to two independent input pulses of frequencies $f_1 = 2\,\text{Hz}$ and $f_2 = 3\,\text{Hz}$. Besides these harmonic signals, we have also considered inharmonic inputs for which the frequencies f_1 and f_2 were equally shifted by an amount Δf. The pools consist of 256 independent neurons modeled by the Morris and Lecar equations (Morris and Lecar, 1981). To account for a more realistic situation we allow for a certain heterogeneity between the neurons (see model description below). Under this situation we observe that the neurons respond to the complex inputs at a ghost frequency that scales linearly with Δf when both inputs are subthreshold, as predicted by Chialvo et al. (2002) in a much simpler single-neuron model. We refer to subthreshold inputs when any of them applied alone do not produce any response from the pool of neurons. When one of the inputs is suprathreshold we still observe the ghost resonance, similar to the case of subthreshold signals, but pulsations of the pool related with the frequency of the suprathreshold signal also appear.

2. Model description

2.1. Neural model

As announced above, we study a configuration consisting in a pool of 256 neurons receiving synaptic inputs from two input neurons, representing two different pathways (see Fig. 1). The dynamical behavior of the membrane potential of each neuron is described by the Morris–Lecar model (Morris and Lecar, 1981):

$$\frac{dV_i}{dt} = \frac{1}{C_m}(I_i^{app} - I_i^{ion} - I_i^{syn}) + D_i\xi(t) \quad (1)$$

$$\frac{dW_i}{dt} = \phi\Lambda(V_i)[W_\infty(V_i) - W_i] \quad (2)$$

where V_i and W_i stand for the membrane potential and the fraction of open potassium channels, respectively. The subindex i labels the different neurons, with $i = 1, 2$ representing the two input neurons and the subsequent $i = 3, \ldots, 258$ representing the neurons of the processing pool. C_m is the membrane capacitance per unit area, I_i^{app} is the external applied current, and I_i^{syn} is the synaptic current. The ionic current is given by

$$I_i^{ion} = g_{Ca}M_\infty(V_i)(V_i - V_{Ca}^0) + g_K W_i(V_i - V_K^0) + g_L(V_i - V_L^0) \quad (3)$$

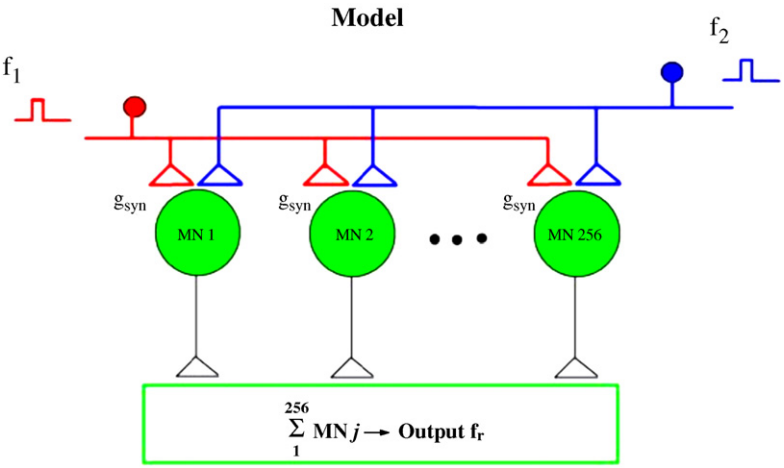

Fig. 1. Schematic diagram of the neuronal configuration studied in this paper.

where g_a (a = Ca, K, L) are the conductances and V_a^0 the resting potentials of the calcium, potassium and leaking channels, respectively. The following functions of the membrane potential are also defined:

$$M_\infty(V) = \frac{1}{2}\left[1 + \tanh\left(\frac{V - V_{M1}}{V_{M2}}\right)\right] \quad (4)$$

$$W_\infty(V) = \frac{1}{2}\left[1 + \tanh\left(\frac{V - V_{W1}}{V_{W2}}\right)\right] \quad (5)$$

$$\Lambda(V) = \cosh\left(\frac{V - V_{W1}}{2V_{W2}}\right), \quad (6)$$

where V_{M1}, V_{M2}, V_{W1} and V_{W2} are constants specified in Table 1 (Tsumoto et al., 2006). The last term in the equation of the membrane potential is a Gaussian white noise of zero mean and intensity D_i, uncorrelated between neurons, and non-zero only for the neurons of the processing pool.

The two input neurons are modulated with harmonic suprathreshold currents with different frequencies f_1 and f_2:

$$I_i^{app} = I_{0i}^{app} + A_i \cos(2\pi f_i t), \quad i = 1, 2. \quad (7)$$

We used the frequencies $f_1 = 2\,\text{Hz} + \Delta f$ and $f_2 = 3\,\text{Hz} + \Delta f$, with $\Delta f = 0$ representing the harmonic case. The bias current is $I_{0,pool}^{app} = 2.2\,\text{mA}$ for the neurons of the pool and $I_{01}^{app} = I_{02}^{app} = 25\,\text{mA}$ for the input neurons, the pulse amplitudes being $A_{1,2} = 24\,\text{mA}$ for both frequencies. With this configuration, the two input neurons generate two periodic spike trains, one with frequency f_1 and the other with frequency f_2, converging on the pool of 256 neurons.

2.2. Synapse model

We represent the coupling between the input and pool neurons with a standard model of chemical synapsis (Destexhe et al., 1994). In this model, coupling is unidirectional from input to pool neurons. The synaptic current acting on neuron i is given by

$$I_i^{syn} = \sum_{j=1,2} g_i^{syn} r_j (V_i - E_s), \quad i = 3, \ldots, 258, \quad (8)$$

where the sum runs over the two input neurons, g_i^{syn} are the conductances of the postsynaptic channels, r_j stands for the fraction of bound receptors of the synaptic channel, V_i is the postsynaptic membrane potential and E_s is a parameter whose value determines the type of synapse. In the present case we assume $E_s = 0\,\text{mV}$ for all synapses, corresponding to all-excitatory couplings. As shown below, ghost resonance does not require inhibitory connections. However, inhibitory synapses do exist in real neuronal networks, and therefore it would be interesting to examine their effect on the behavior reported below.

Table 1
Parameters values of the Morris–Lecar and synapse models used in this work

Parameters	Value
C_m	$5\,\mu\text{F/cm}^2$
V_K	$-80\,\text{mV}$
V_L	$-60\,\text{mV}$
V_{Ca}	$120\,\text{mV}$
V_{M1}	$-1.2\,\text{mV}$
V_{M2}	$18\,\text{mV}$
V_{W1}	$2\,\text{mV}$
V_{W2}	$17.4\,\text{mV}$
ϕ	$1/15\,\text{s}^{-1}$
g_K	$8\,\mu\text{S/cm}^2$
g_L	$2\,\mu\text{S/cm}^2$
g_{Ca}	$4\,\mu\text{S/cm}^2$
α	$0.5\,\text{ms}^{-1}$
β	$0.1\,\text{ms}^{-1}$
g_{syn}	See text
τ_{syn}	35 ms
E_s	0 mV

The fraction of bound receptors, r_j, obeys the equation:

$$\frac{dr_j}{dt} = \alpha[T]_j(1 - r_j) - \beta r_j, \quad (9)$$

where $[T]_j = \theta(T_0^j + \tau_{syn} - t)\theta(t - T_0^j)$ is a square pulse of width τ_{syn} representing the concentration of neurotransmitter released in the synaptic cleft, α and β are rise and decay time constants, respectively, and T_0^j is the time at which the presynaptic neuron j fires, which happens whenever the presynaptic membrane potential exceeds a predetermined value, in our case chosen to be 0 mV. The values of the used parameters are also specified in Table 1 and were taken from Destexhe et al. (1994).

2.3. Numerical protocols

We perform two kinds of numerical experiments. In the first, we set the excitation level of the pool neurons and the synaptic coupling between those and the input neurons to values for which the stimuli are subthreshold if they arrive separately to each pool neuron, and suprathreshold if they arrive together. We also introduce heterogeneity in the pool of processing neurons by adding a 10% variability to their applied current (I_{pool}^{app}) and choosing a synaptic conductance between input and pool neurons with average value $g_{pool}^{syn} = 1.2\,\text{nS/cm}$ and

20% variability. We also add a small quantity of white noise with amplitude $D_{\text{pool}} = 0.5\,\text{mV/ms}$ to the pool neurons. Due to the heterogeneity some neurons do not fire even when two inputs arrive together. Thus, most of the pool neurons (but not all) act as coincidence detectors from the spikes coming from the different inputs.

In the second type of simulations, we introduce another source of heterogeneity by considering that the neurons respond differently to the different inputs. Specifically, we choose $g^{\text{syn}}_{\text{pool}} = 1.0\,\text{nS/cm} \pm 20\%$ if the input comes from neuron 1 (spiking with frequency f_1) and $g^{\text{syn}}_{\text{pool}} = 1.8\,\text{nS/cm} \pm 20\%$ if the input comes from neuron 2. We also consider a higher noise level for the neurons in the pool, with amplitude $D_{\text{pool}} = 2.0\,\text{mV/ms}$.

The equations where integrated using the Heun method (García-Ojalvo and Sancho, 1999), which is equivalent to a second order Runge-Kutta algorithm for stochastic equations.

3. Results

We have numerically studied the two situations described above, using the parameters given in Table 1. We consider different pairs of input frequencies $f_1 = kf_0 + \Delta f$ and $f_2 = (k+1)f_0 + \Delta f$, with $f_0 = 1\,\text{Hz}$ and $k > 1$, and increase both frequencies simultaneously in steps of Δf. For each pair of frequencies, we run simulations over a time span of 60 s, with a time step of 0.01 ms.

3.1. All neurons subthreshold

In this situation, no neuron in the pool is suprathreshold to a single input. We start analyzing the harmonic case, when the input neurons are spiking with frequencies $f_1 = 2\,\text{Hz}$ and $f_2 = 3\,\text{Hz}$. These frequencies are higher-order harmonics of $f_0 = 1\,\text{Hz}$, which is also their frequency difference. Those neurons in the pool that receive both inputs at the same time produce a spike, provide the combined stimulation is above threshold. Fig. 2 shows, in its top panel, the average membrane potential of the pool as a function of time. Spikes in the average membrane potential are clearly observed with a period of 1 s, corresponding with the ghost fundamental frequency $f_0 = 1\,\text{Hz}$. These spikes are interspersed with small-amplitude depolarization episodes that cannot be considered action potentials. A corresponding raster plot, shown in the bottom panel of Fig. 2 is constructed by defining a spike when the single-neuron membrane potential surpasses a threshold $V_{\text{thr}} = 0\,\text{mV}$. The response at the ghost frequency is evident from this plot.

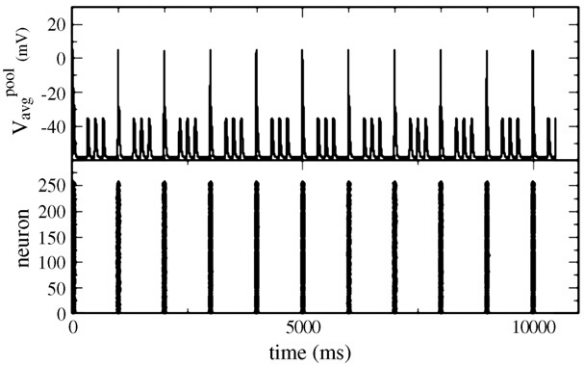

Fig. 2. Average membrane potential of the pool of neurons (upper panel) and raster plot (lower panel) when the neurons of the pool are subthreshold to separately arriving inputs.

Next we analyze the case in which the input signals keep their frequency difference ($f_0 = 1\,\text{Hz}$), but they are no longer higher-order harmonics of f_0, i.e. $f_1 = kf_0 + \Delta f$ and $f_2 = (k+1)f_0 + \Delta f$. In order to analyze the response of the pool, we consider the average membrane potential plotted above for each pair of frequencies and calculate the instantaneous firing rate f_{r} as the inverse of the time between consecutive spikes along each time series. Fig. 3 shows the distribution of response frequencies f_{r} as a function of the input frequency f_1 (with $f_2 = f_1 + f_0$ in every case). One can observe that most of the responses follow the relation predicted by Chialvo et al. (2002) for sinusoidal inputs, reproduced by Balenzuela and García-Ojalvo (2005) for spiking inputs, and observed in the psycho-acoustical experiments of Schouten et al. (1962):

$$f_{\text{r}} = f_0 + \frac{\Delta f}{k + 1/2}. \tag{10}$$

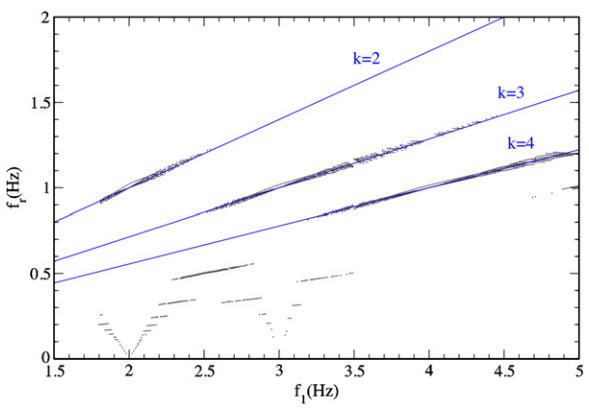

Fig. 3. Distribution of response frequencies f_{r} (inverse of the interspike intervals of the average membrane potential) as a function of the input frequency $f_1 = kf_0 + \Delta f$. In this case all neurons in the pool are subthreshold to inputs arriving separately.

This expression corresponds to a linear relation between f_r and Δf (and hence f_1), which is represented in Fig. 3 by means of lines for different values of k. Fig. 3 also reveals responses at much lower frequencies, which are characteristic of the detection of coincidences of inharmonic input pulses (see, for instance, Lopera et al., 2006).

3.2. Some neurons suprathreshold

The results described above show that the simple mechanism of ghost resonance, previously reported for the combination of sinusoidal (Chialvo et al., 2002) and spiking (Balenzuela and García-Ojalvo, 2005) inputs in single-neuron models, persists in the more realistic case in which input signals act upon a pool of heterogeneous neurons. However, it's reasonable to anticipate that in an experimental setting it will be difficult to adjust the input signals in such a way that all neurons in the processing pool are below threshold. Therefore the question arises of what is the behavior of the system when a fraction of the neurons in the pool is suprathreshold for at least one of the two inputs.

To answer that question, we now consider that the input coming from neuron 2 is stronger than the one coming from neuron 1 (see Fig. 1), so that some neurons are suprathreshold to the synaptic input coming from neuron 2 with frequency f_2. The resulting time series of the average membrane potential is shown in the top panel of Fig. 4. Again a response at the ghost frequency is clearly revealed by high-amplitude spikes, but this response is now interspersed with depolarization events at frequency f_2 which are considerable more intense than in the case where all neurons in the pool are assumed to be subthreshold (compare this plot with Fig. 2). Note that, as shown in the raster plot appearing in the bottom panel of Fig. 4, a sizable fraction of the neurons are suprathreshold with respect to the input f_2 (compare the bottom panels of Figs. 2 and 4). In other words, while most of the neurons spike at the ghost frequency (every 1 s), some neurons fire with frequency $f_2 = 3$ Hz coming from one of the inputs.

Due to the relatively high amplitude of the depolarization events at the input frequency f_2, shown as middle-sized spikes in the top panel of Fig. 4, differences may arise when analyzing the corresponding time series of the average membrane potential, depending on the threshold being used to define when spikes take place. For instance, for a high enough threshold (upper horizontal line in the top panel of Fig. 4) only the ghost

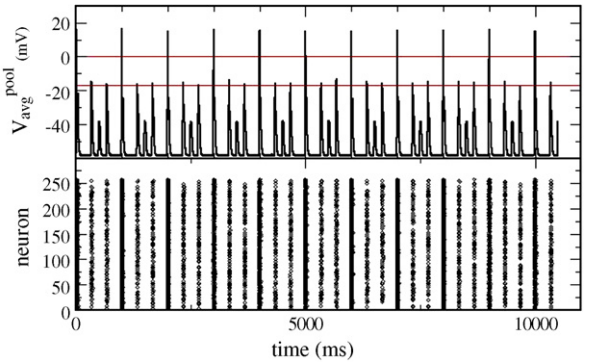

Fig. 4. Average membrane potential of the pool of neurons (upper panel) and raster plot (lower panel) when some of the neurons of the pool are suprathreshold to the input coming from neuron 2 (with frequency f_2). The horizontal lines in the upper panel denote two different thresholds used to compute the probability distributions of response frequencies, such as those shown in Fig. 5. The raster plot has been computed by applying a threshold $V_{thr} = 0$ mV to the individual membrane potentials of the neurons.

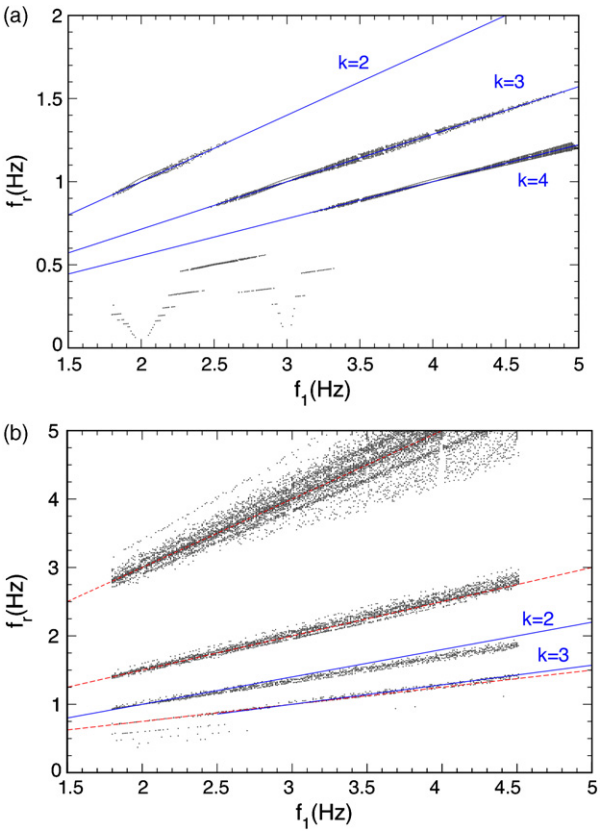

Fig. 5. Distribution of response frequencies f_r (inverse of the interspike intervals of the average membrane potential) as a function of the input frequency $f_1 = kf_0 + \Delta f$, when some of the neurons of the pool are suprathreshold with respect to the input coming from neuron 2 (with frequency f_2). Left: high spike threshold; right: low spike threshold. Note the difference between the scales of the vertical axis in the two plots.

frequency $f_0 = 1$ Hz is detected. On the other hand, when the threshold is smaller (lower horizontal line in the plot), the input frequency $f_2 = 3$ Hz is usually detected, while depending on the noise level the ghost frequency arises as well.

Certainly, the interpretation problems highlighted above also persist in the case of inharmonic inputs, i.e. when the input frequencies are detuned by a frequency shift Δf while keeping their frequency difference constant. Fig. 5 represents the distribution of instantaneous firing rates f_r as a function of one of the input frequencies f_1, with $f_2 = f_1 + f_0$. When a high threshold is used to determine the existence of a spike (upper horizontal line in the top panel of Fig. 4), the corresponding response-frequency distribution (left panel of Fig. 5) looks very similar to the case in which all neurons are subthreshold (Fig. 3). This happens because only the spiking events associated with successful detection coincidences are identified in this case, while the neurons responding directly at frequency f_2 do not have an effect on the measure defined above. But if the threshold is smaller (lower horizontal line in the top panel of Fig. 4), new frequencies arise in the distribution plot, corresponding to $f_r = f_2 + \Delta f$ and its subharmonics (red dashed lines in the right plot of Fig. 5). In other words, the system detects not only the ghost frequency, but also the input frequency at which some of the neurons in the pool are suprathreshold.

4. Discussion

Many basic studies and predictions in neuronal dynamics are based on models of single neurons. An example is the subharmonic response to a complex signal known as ghost resonance, which was first proposed by Chialvo et al. (2002) for a combination of harmonic tones acting on an isolated neuron, and was later extended to the case of spiking inputs by Balenzuela and García-Ojalvo (2005). In the latter case, the phenomenon took the form of a coincidence-detection mechanism.

However, real experimental investigations of dynamical processes in neuronal circuits frequently involve pools of many neurons, which furthermore present a substantial level of heterogeneity. It is thus necessary to determine (i) whether ghost resonance prevails in that case, and (ii) what is the influence of heterogeneity on the system's response. The present study addresses these two issues, and in relation with the second one it shows that different results can be obtained depending on how the system's behavior is quantified. Specifically, heterogeneity in the thresholds of the different neurons in the pool may lead to spike time distributions that reveal the main hallmarks of ghost resonance, but which nevertheless may or may not exhibit other responses depending on how a spike in the average membrane potential (which is the quantity that frequently has a functional role) is "defined". Of course, the answer to this question will depend on the physiological responses that the neuronal processing pool is expected to elicit. Therefore, it is important to take the preceding considerations into account when designing an experiment to test the validity of the ghost-resonance mechanism, and in general of any mechanism based on coincidence detection.

Acknowledgements

We acknowledge Javier M. Buldú for helpful discussions. Financial support has been provided by Ministerio de Educación y Ciencia (Spain) and FEDER through projects BFM2003-07850 and FIS2004-00953, and ORDEN by the Generalitat de Catalunya. P.B. is a member of "Carrera de Conicet", Argentina, and was supported by a fellowship C-RED of the Generalitat de Catalunya.

References

Balenzuela, P., García-Ojalvo, J., 2005. Neural mechanism for binaural pitch perception via ghost stochastic resonance. Chaos 15, 023903.

Buldú, J., Chialvo, D., Mirasso, C., Torrent, M., García-Ojalvo, J., 2003. Ghost resonance in a semiconductor laser with optical feedback. Europhys. Lett. 64, 178–184.

Buldú, J.M., González, C.M., Trull, J., Torrent, M.C., García-Ojalvo, J., 2005. Coupling-mediated ghost resonance in mutually injected lasers. Chaos 15, 013103.

Calvo, O., Chialvo, D.R., 2006. Ghost stochastic resonance in an electronic circuit, Int. J. Bif. Chaos. 16, 731-735.

Chialvo, D., 2003. How we hear what is not there: a neural mechanism for the missing fundamental illusion. Chaos 13, 1226–1230.

Chialvo, D., Calvo, O., González, D., Piro, O., Savino, G., 2002. Subharmonic stochastic synchronization and resonance in neuronal systems. Phys. Rev. E 65 050902(R).

Destexhe, A., Mainen, Z., Sejnowski, T., 1994. An efficient method for computing synaptic conductances based on a kinetic model of receptor binding. Neural Comput. 6, 14–18.

García-Ojalvo, J., Sancho, J.M., 1999. Noise in Spatially Extended Systems. Springer-Verlag, New York.

Lopera, A., Buldú, J., Torrent, M., Chialvo, D., García-Ojalvo, J., 2006. Ghost stochastic resonance with distributed inputs in pulse-coupled electronic neurons. Phys. Rev. E 73, 021101.

Manjarrez, E., Balenzuela, P., Garcia-Ojalvo, J., Vasquez, E.E., Martinez, L., Flores, A., Mirasso, C.R., 2006. Phantom reflexes: Muscle contractions at a frequency not physically present in the input stimuli. Biosystems, doi:10.1016/j.biosystems.2006.10.002, in press.

Morris, C., Lecar, H., 1981. Voltage oscillations in the barnacle giant muscle fiber. Biophys. J. 35, 193–213.

Pantev, C., Elbert, T., Ross, B., Eulitz, C., Terhardt, E., 1996. Binaural fusion and the representation of virtual pitch in the human auditory cortex. Hearing Res. 100, 164–170.

Schouten, J.F., Ritsma, R., Cardozo, B.L., 1962. Pitch of the residue. J. Acoust. Soc. Am. 34, 1418–1424.

Tsumoto, K., Kitajima, H., Yoshinaga, Y., Aihara, K., Kawakami, H., 2006. Bifurcations in Morris–Lecar neuron model. Neurocomputing 69, 293–316.

Van der Sande, G., Verschaffelt, G., Danckaert, J., Mirasso, C., 2005. Ghost stochastic resonance in vertical-cavity surface-emitting lasers: experiment and theory. Phys. Rev. E 72, 016113.